

excludes the other, and they may be taken together in order to reduce the calculated nucleation field.

In Sec. I, it was assumed that $\rho_i < 1$ (for $i = 1, 2$), but from the equations (6) and (9) we can see that, if it is assumed $\rho_i > 1$, the calculated nucleation field remains the same as plotted in Fig. 1 for the same value of ρ . This means that the exchange energy and the magnitude of the magnetization vector can be assumed to be larger

in the surface layer than in the bulk and still the calculated nucleation field is lower.

ACKNOWLEDGMENTS

I am greatly indebted to Professor E. H. Frei and Dr. A. Aharoni, under whom this work has been carried out.

High-Temperature Series Expansions for the Spin- $\frac{1}{2}$ Heisenberg Model by the Method of Irreducible Representations of the Symmetric Group*

GEORGE A. BAKER, JR.

University of California, Los Alamos Scientific Laboratory, Los Alamos, New Mexico

AND

G. S. RUSHBROOKE

Physics Department, King's College, Newcastle-upon-Tyne, England

AND

H. E. GILBERT

University of California, Los Alamos Scientific Laboratory, Los Alamos, New Mexico

(Received 3 April 1964)

We show how the partition functions for finite clusters with spin- $\frac{1}{2}$ Heisenberg interactions may be computed efficiently and generally to any desired number of powers in reciprocal temperature. As an example, we have expanded the zero-magnetic-field free energy to the twenty-first power for the linear Heisenberg model and for nonzero magnetic field give an expression good through the tenth power. We introduce the concept of the two-point Padé approximant and use it to analyze the energy for the linear Heisenberg model.

1. INTRODUCTION AND GENERAL THEORY

RECENT advances in the ability of experimental physicists to measure the nature of the singularity in various thermodynamics functions near the critical point have raised anew the question of the adequacy of the Heisenberg model of magnetism to describe real substances in the critical region.¹ Studies by various authors² have shown that in the analogous Ising model, the most precise method now known of determining the predictions of models of this sort is the analysis of the exact power-series expansions (in reciprocal temperature, etc.) of the various thermodynamic functions. The major problem involved in extending the power series for the Heisenberg model has been the calculation of the traces of the spin operators involved. In this section of our paper we show how that step can be

greatly simplified and easily adapted for a computer. In the last section of our paper we will apply our method, as an example, to the linear Heisenberg model, and analyze, by means of the Padé approximant method, the energy and magnetic susceptibility. We digress in the second section to introduce the concept of the 2-point Padé approximant, which turns out to be extremely useful in discussing the linear ferromagnetic Heisenberg model.

Domb³ has pointed out that the partition function of an infinite lattice can be simply expressed in terms of the partition functions for finite clusters. That this procedure is possible follows from the fact that the logarithm of the partition function for a general lattice can be written in the form

$$\ln Z^{(j)} = \sum_{\alpha} p_{\alpha}^{(j)} \varphi_{\alpha}, \quad (1.1)$$

where α denotes a connected graph, $p_{\alpha}^{(j)}$ is the number of distinct ways it occurs on lattice (j), and φ_{α} is a unique function associated with graph α . By applying (1.1) successively to various finite clusters we may solve for the φ_{α} 's, and then, knowing the lattice constants

* Work supported in part by the U. S. Atomic Energy Commission.

¹ J. L. Gammel, W. Marshall, and L. Morgan, Proc. Roy. Soc. (London) **A275**, 257 (1963).

² See, e.g., G. A. Baker, Jr., Phys. Rev. **124**, 768 (1961); **129**, 99 (1963); J. W. Essam and M. E. Fisher, J. Chem. Phys. **38**, 802 (1963); M. F. Sykes and M. E. Fisher, Physica **28**, 919, 939 (1962); M. F. Sykes and C. Domb, J. Math. Phys. **2**, 52, 63 (1961).

³ C. Domb, Phil. Mag. Suppl. **9**, 149 (1960), p. 330.

for an infinite lattice, obtain an expression for its partition function in terms of the φ_α 's. Since φ_α is proportional to $K^{l+\lambda}$, where l is the number of lines in α , and $\lambda \geq 0$, we may exhaustively catalog all the α 's required to obtain the expansion of the partition function to a given power of K .

Normally, using the finite cluster method, one is confronted with the problem of taking the traces of powers of $2^N \times 2^N$ matrices, where N is the number of spins in the cluster. For 10th order, open, connected configurations N can be 11 and so we get 2048×2048 matrices. Since the labor in computing a power of a matrix is proportional to the cube of its order, we get about 10^{10} operations per power, a formidable task even for the fastest computers available today. We can simplify the task in the following way: The Hamiltonian is

$$\mathfrak{H} = -\frac{1}{2}J \sum_{\text{nearest neighbors}} \boldsymbol{\sigma}_i \cdot \boldsymbol{\sigma}_j - (\mu H) \sum_{\text{cluster}} \sigma_{zi}, \quad (1.2)$$

where the $\boldsymbol{\sigma}_i$ are the vectors of Pauli spin matrices associated with site i . The partition function is

$$Z(\beta, H) = \text{Tr}[\exp(-\beta\mathfrak{H})]. \quad (1.3)$$

As the parts of the Hamiltonian represented by the first and second sum commute, they must be simultaneously diagonalizable. The subspaces in which the second sum has degenerate eigenvalues are very simple. They are spanned by the $\binom{N}{m}$ vectors with m spins down and all other spins up. Hence, the entire Hamiltonian (and all powers of it) must be decomposable into block matrices of dimension at most $\binom{N}{m}$. For the 11 spin case, the order of the largest block is now reduced from 2048 to 462.

A further comparable reduction in block size is possible on the basis of the following observation. The Dirac relation,

$$(\boldsymbol{\sigma}_i \cdot \boldsymbol{\sigma}_j) = 2P_{ij} - I, \quad (1.4)$$

tells us that $(\boldsymbol{\sigma}_i \cdot \boldsymbol{\sigma}_j)$, even in a 2048×2048 representation, is a linear combination of the permutation operator P_{ij} and the identity operator I . By the well-known results of group theory, any representation of the symmetric group may be broken down into irreducible representations of the symmetric group. Following the analysis of Wigner⁴ we can easily break down the representation into its proper irreducible components. If $\Delta^{(k)}(R)$ is the submatrix with all but k spins up, which represents permutation R , then the corresponding eigenvalue of $\sum_i \sigma_{zi}$ is $(N - 2k)$. Furthermore, according to Wigner,³ this representation is reducible as

$$\Delta^{(k)}(R) = \Delta^{(k-1)}(R) + D^{(k)}(R), \quad (1.5)$$

where $k \leq N/2$, and $D^{(k)}(R)$ is an irreducible representation of R of dimension $\binom{N}{k} - \binom{N}{k-1}$, and $\binom{N}{k}$ is the usual

⁴ E. P. Wigner, *Group Theory and its Application to the Quantum Mechanics of Atomic Spectra*, translated by J. J. Griffin (Academic Press Inc., New York, 1959), Chap. 13.

binomial coefficient. For $k > \frac{1}{2}N$, $\Delta^{(N-k)}(R)$ is related by a similarity transform to $\Delta^{(k)}(R)$. Thus, due to the repetition of the $D^{(k)}(R)$, the maximum block size is reduced (for $N=11$ to 165) and there are the same number of representations as before this reduction was performed. The partition function, (1.3), for a finite cluster is given exactly by

$$Z(\beta, H) = \sum_{L=0}^{\infty} \frac{(\frac{1}{2}\beta J)^L}{L!} \left\{ \sum_{k=0}^{[N/2]} \text{Tr}(\Gamma_k^L) \times \sum_{m=k}^{N-k} e^{(N-2m)\beta\mu H} \right\}, \quad (1.6)$$

where Γ_k is the matrix representative of $\sum_{\text{cluster}} (2P_{ij} - I)$ in the k th irreducible representation, $[]$ denotes the greatest integer, and $\text{Tr}(X)$ is the trace or character of X . These irreducible representations, in the Young tableaux description, are those irreducible representations with at most two horizontal rows and contain exactly k squares in the second row. As the matrix representatives for permutations on N items are easily constructed in terms of those for $N-1$ and $N-2$ items by following the standard prescription,⁵ we will not belabor it here. The special case of (1.6) for $H=0$,

$$Z(\beta, 0) = \sum_{L=0}^{\infty} \frac{(\frac{1}{2}\beta J)^L}{L!} \left\{ \sum_{k=0}^{[N/2]} \text{Tr}(\Gamma_k^L) (N-2k+1) \right\} \quad (1.7)$$

has been given previously by Wood and Pirnie.⁶

2. TWO-POINT PADÉ APPROXIMANT

The Padé approximant $[M, N]$ is the ratio of two polynomials $P_N(z)/Q_M(z)$ of degrees N and M . The coefficients are chosen so that the power-series expansion of the quotient agrees with that of the function through the term z^{M+N} . These approximants have proven powerful in the inference of quantitative information from power-series coefficients and from qualitative information about the analytic structure of the function.⁷

Sometimes it happens that one has information about a function at two (or more) points. We propose to take it into account by requiring the Padé approximant to satisfy exactly the condition at the second point as well as those at the first, which is the origin. In the examples we will discuss, we impose the value of the function at infinity on the $[N, N]$ Padé approximants. The required modification in the linear equations which determine the coefficients of P and Q is slight. One replaces the equation, which makes the last power-

⁵ See, for instance, M. Hamermesh, *Group Theory and its Application to Physical Problems* (Addison-Wesley Publishing Company, Inc., Reading, Massachusetts, 1962), Chap. 7, especially Sec. 7.7.

⁶ P. J. Wood and K. Pirnie (private communication).

⁷ See the papers of Ref. 2 and the works referred to therein for a fuller discussion of the Padé approximant method.

series term agree, by one which makes the Padé approximant equal to a given value at infinity. We have run a few cases to illustrate the nature of the results which might be obtained and to indicate what may and may not reasonably be expected of this method. We have considered

$$\begin{aligned} a(x) &= 1 - \exp(-x), \\ u(x) &= (1+x^2)^{1/2}/(1+x), \\ c(x) &= [(1+x+x^2)^{1/2}-1]/x. \end{aligned}$$

The standard $[N,N]$ Padé approximants do not converge to $a(\infty)$,⁸ because infinity is an essential singularity, but oscillate 0, 2, 0, 2, 0, \dots , indefinitely. When the value $a(\infty)=1.0$ is fixed, then the $[N,N]$ Padé approximants converge rapidly. The $[7,7]$ gives $a(5)$ to one part in 10^5 and more accurately for smaller real arguments. The most inaccurate region is for large but not infinite arguments where there can occur errors of about one percent. This represents a substantial improvement in the large argument region over the standard Padé approximant as pointed out above. In this example we have used the two-point method to specify the value at an essential singularity.

For the function $u(x)$ the point at infinity lies on the branch cut⁸ connecting the two branch points at $\pm i$, when we use the cut convention defined by the $[N,N]$ Padé approximants. Continuing from positive or negative real values of x , we get $+1$ and -1 , respectively, for $u(\infty)$. When we specify $+1$ as the asymptotic value, all the poles and zeros by which the $[N,N]$ Padé approximants simulate a branch cut lie in the left-half plane. $u(1)$ is given by the $[8,8]$ approximant to better than one part in 10^6 and for smaller real positive arguments the accuracy is better. For larger arguments the accuracy decreases to about two percent in the range $10 \leq x \leq 30$ and, of course, then increases to zero error at $x = \infty$.

If we specify $u(\infty) = -1$, then all the poles and zeros simulating the branch cut are in the right-half plane. If we now consider negative real values of x , the accuracy picture is much the same as it was for the positive case of $u(x)$. The pole at $x = -1$ is located to within 3 parts in 10^6 by the $[8,8]$ approximant. The maximum error is about 3% here. For the function $u(x)$ we have used the two-point method to specify which lip of a branch cut for the approximant to converge to.

The function $c(x)$ has branch points at $x = -\frac{1}{2} \pm i\sqrt{\frac{3}{4}}$. The standard Padé approximant would cut⁸ this function so as to connect these branch points and form a single-valued function. The branch cut would cross the real axis at $x = -2$. If we continue through this cut along the negative real axis, we obtain $c(-\infty) = -1$. If we continue along the positive real axis, we

obtain $c(+\infty) = +1$, the branch given by the standard $[N,N]$ Padé approximants. When we fix the value $c(\infty) = 1$, we specify the value at a regular point and do not much perturb the structure of the approximants, except to greatly accelerate convergence in the neighborhood of that regular point. The $[5,5]$ for this case is good to better than one part in 10^4 for all positive real x .

When we specified $c(\infty) = -1$ in an effort to cause the $[N,N]$ Padé approximants to choose the other branch in the region of large negative x , we were not especially successful. Although through the $[2,2]$ Padé approximant, it appeared as though the desired branch was being taken, as we went to higher approximants the branch cut was made in the same general way as before and, in fact, the $[5,5]$ Padé approximant does not become negative until $|x| > 170$. We see from this example that specification at a regular point works very well, but that specifying the value alone, does not cause the $[N,N]$ Padé approximants to change their "natural" Riemann sheet. It may be that with a more nearly balanced ratio between coefficients given at zero and infinity one could force a change of what is the "natural" Riemann sheet, but we have not investigated this point.

3. THE LINEAR HEISENBERG MODEL

In order to illustrate our method we have obtained an expression from which one can calculate the series expansion for the linear Heisenberg model through the tenth order in $K = \frac{1}{2}\beta J$ and all orders in $\bar{H} = \beta\mu H$. For $H = 0$ we obtain the 21st order in K . The counting problem is elementary here. If (j) denotes a linear chain of j links then the $p_\alpha^{(j)}$ of Eq. (1.1) become

$$\begin{aligned} P_\alpha^{(j)} &= j+1-\alpha, & \alpha \leq j \\ &= 0, & \alpha > j \end{aligned} \tag{3.1}$$

and for the infinite linear model

$$\lim_{N \rightarrow \infty} [\ln Z^{(N)}/N] = \sum_{\alpha=1}^{\infty} \varphi_\alpha. \tag{3.2}$$

If we know the exact partition functions for finite clusters through ten links, then we obtain

$$\sum_{\alpha=1}^{10} \varphi_\alpha = \ln Z^{(10)} - \ln Z^{(9)}. \tag{3.3}$$

The φ_α for the linear graphs are unusual in that they are proportional to $(K)^{2\alpha}$ rather than K^α as are, for example, the φ 's associated with simple closed polygons. This means that the first ten φ_α 's suffice to give 21 terms in the zero-field expansion of the partition function. In a nonzero magnetic field the φ_α are again proportional to K^α and in particular we can only obtain the magnetic susceptibility through K^{10} from ten φ_α 's. The proof of this unusual property of the linear clusters is easily given. If we stop at the n -point chain,

⁸ G. A. Baker, Jr., J. L. Gammel, and J. G. Wills, *J. Math. Analysis App.* **2**, 405 (1961).

TABLE I. $\text{Tr}(\Gamma_k^L)$.

$L \setminus k =$	0	1	2	3	4	5	
			$(j=9)$				
0	1	9	35	75	90	42	
1	9	45	63	-45	-198	-126	
2	81	289	651	1755	3034	1722	
3	729	2085	2919	-4605	-21 414	-15 246	
4	6561	15 929	26 355	99 435	293 210	210 762	
5	59 049	125 725	158 223	-506 445	-3172 358	-2697 246	
6	531 441	1013 329	1340 763	7915 515	43 207 642	39 837 402	
7	4782 969	8287 765	9275 959	-58 431 005	-557 643 494	-592 359 726	
8	43 046 721	68 522 089	76 729 795	773 505 163	7814 375 002	9273 490 026	
9	387 420 489	571 285 005	573 903 327	-7029 326 445	-109 145 995 590	-147 414 544 830	
10	3486 784 401	4794 694 529	4716 628 011	85 971 909 915	1575 964 920 794	2393 875 707 642	
			$(j=10)$				
0	1	10	44	110	165	132	
1	10	60	120	20	-270	-360	
2	100	432	1008	2576	5364	5472	
3	1000	3456	6240	-640	-30 840	-46 080	
4	10 000	29 312	52 160	139 136	486 224	677 120	
5	100 000	257 280	401 280	-190 720	-4666 080	-8578 560	
6	1000 000	2308 224	3408 384	10 037 120	67 609 920	131 632 896	
7	10 000 000	21 024 000	28 511 232	-29 383 936	-822 459 264	-1986 734 592	
8	100 000 000	193 626 112	247 929 856	857 096 192	11 798 357 248	32 177 373 184	
9	1000 000 000	1798 447 104	2162 104 320	-3964 248 064	-160 690 048 512	-527 081 914 368	
10	10 000 000 000	16 817 027 072	19 202 244 608	82 144 987 136	2342 240 605 183	8898 064 781 309	


we are omitting Brout graphs from the free-energy expansion for which the basic graphs⁹ are chains of n or more links. Thus, the first error in the series arises from Brout graphs based on the basic graph in Fig. 1. But the first such nonvanishing Brout graph is shown in Fig. 2, and has $2n$ links. This is because, associated with any Brout graph is the corresponding cumulant, and any cumulant is the sum of products of moments of subgraphs (partitions of the lines in the Brout graph). However, the moment of any such graph having an undoubled link vanishes.¹⁰

For a nonzero magnetic field, the partition function

$$\begin{aligned} \ln Z^{(10)} - \ln Z^{(9)} \simeq & (\ln Z^{(\infty)} / \infty) \simeq \ln 2 + 3K^2/(2!) - 6K^3/(3!) - 30K^4/(4!) + 360K^5/(5!) + 504K^6/(6!) \\ & - 44\,016K^7/(7!) + 204\,048K^8/(8!) + 8261\,760K^9/(9!) - 128\,422\,272K^{10}/(10!) - 1816\,480\,512K^{11}/(11!) \\ & + 7656\,2054\,400K^{12}/(12!) + 1.24207469568 \times 10^{11}K^{13}/(13!) - 5.1042832542 \times 10^{13}K^{14}/(14!) + 5.8068671970 \\ & \times 10^{14}K^{15}/(15!) + 3.6632422458 \times 10^{16}K^{16}/(16!) - 1.14118428294 \times 10^{18}K^{17}/(17!) - 2.3612862501 \\ & \times 10^{19}K^{18}/(18!) + 1.881307595 \times 10^{21}K^{19}/(19!) + 2.53020316 \times 10^{20}K^{20}/(20!) - 3.04552721 \\ & \times 10^{24}K^{21}/(21!) + \dots + \bar{H}^2[\frac{1}{2} + K - 8K^3/(3!) + 40K^4/(4!) + 336K^5/(5!) - 6384K^6/(6!) - 10\,240K^7/(7!) \\ & + 1461\,888K^8/(8!) - 9566\,720K^9/(9!) - 434\,804\,480K^{10}/(10!) + \dots]. \end{aligned} \quad (3.5)$$

These results agree with those published previously by one of us,¹⁰ and also with those published by Domb⁹ and Wood¹¹ through $K^9\bar{H}^0$ and $K^8\bar{H}^2$.

We have used the standard Padé approximant method² to analyze the magnetic susceptibility. First,

FIG. 1. Basic graph. (n LINKS) 

⁹ G. S. Rushbrooke, J. Math. Phys. 5, 1106 (1964).

¹⁰ G. S. Rushbrooke and P. J. Wood, Mol. Phys. 1, 257 (1958), theorems III and IV.

¹¹ C. Domb and D. W. Wood, Phys. Letters 8, 20 (1964).

per site is given through tenth order in K by

$$\lim_{N \rightarrow \infty} [Z_{\infty}^{(N)}(\beta, H)]^{1/N} = \frac{Z_{10}^{(10)}(\beta, H)}{Z_{10}^{(9)}(\beta, H)} + O(K^{11}), \quad (3.4)$$

where $Z_k^{(j)}(\beta, H)$ is the expansion through k th order given by Eq. (1.6) of the partition function of a cluster of length j . We have tabulated in Table I the traces needed to evaluate Eq. (3.4). We have derived from $Z_{21}^{(10)}$ and $Z_{21}^{(9)}$ the following terms in the series expansion for the free energy per site for an infinite lattice. It is

to determine the nature of the singularity at $K = \infty$ ($T=0$) we have computed the $[N, N+j]$ Padé approximants for $j = -1, 0, +1$ to $[d(\ln \chi)/dK]$, where $\chi = \chi_0/\beta\mu^2$ is the reduced susceptibility. In Fig. 3 we have plotted from the $[N, N-1]$ Padé approximants the values of $K[d(\ln \chi)/dK]$. The limit as K tends to infinity is the power of the reduced magnetic suscepti-

(2n LINKS) 

FIG. 2. First nonvanishing Brout graph based on the basic graph of Fig. 1.

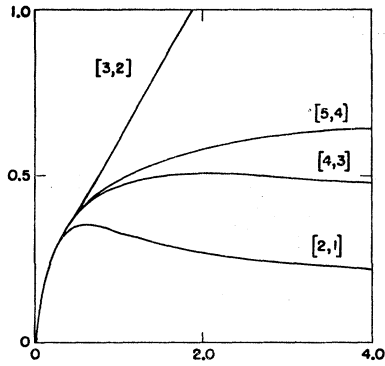


FIG. 3. $K[d \ln z / dK]$ versus K based on the $[N, N-1]$ Padé approximants.

bility singularity. The $[N, N-1]$ were used to obtain the correct asymptotic behavior. The other values of j tend to confirm this curve, and seem to rule out here the exponential behavior which the linear Ising model shows. As can be seen from Fig. 3 the N odd approximants uniformly decrease and the N even uniformly increase. As the values at infinity are

$$\begin{aligned} [2,1] &= 0.1428, \\ [3,2] &= 6.9735, \\ [4,3] &= 0.3627, \\ [5,4] &= 0.7438. \end{aligned} \quad (3.6)$$

We estimate, with the aid of Fig. 3, that the limit is $(\frac{2}{3}) \pm 0.1$. Since the $[4,3]$ rises above 0.5 and the converged portion of the curve shown in Fig. 3 is monotonic, we have selected $\frac{2}{3}$ as the simplest fraction in the allowed range. Using this hypothesis we have calculated

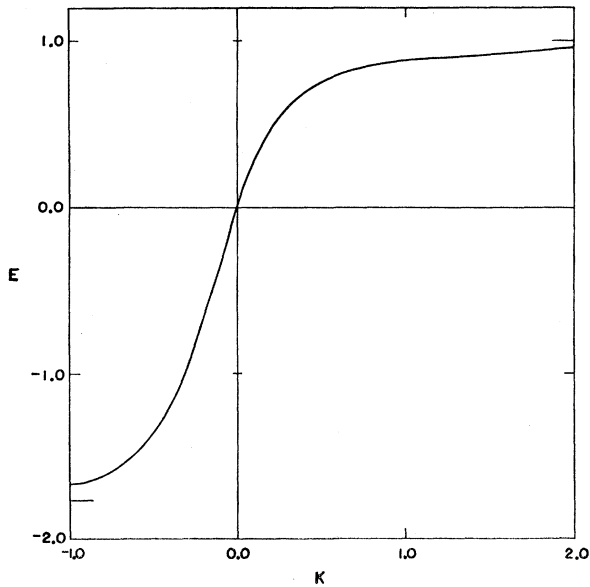


FIG. 4. $E(K)$ based on the $[9,9]$ two-point Padé approximants. The plus side is the ferromagnetic case and the minus side is the antiferromagnetic case. The asymptotic limits are indicated by the large tick marks. E is measured in units of $\frac{1}{2}J$.

the $[N, N+1]$ approximants to $[z(K)]^{3/2}$, as $[z(K)]^{3/2}$ should diverge linearly as $K \rightarrow \infty$. The limit of $[z(K)]^{3/2}/K$ as given by these approximants as K goes to infinity is the coefficient of the singularity. The values obtained are

$$\begin{aligned} [1,2] &= 3.5, \\ [2,3] &= 2.4424, \\ [3,4] &= 3.4158, \\ [4,5] &= 3.0686. \end{aligned} \quad (3.7)$$

These results lead us to speculate that

$$z \approx (\pi K)^{2/3}, \quad (3.8)$$

as K tends to infinity. We wish to emphasize, however, that there must be considered to be about a ten percent error in the coefficient and the power. The error of the $[4,5]$ approximant is apparently less than one percent at

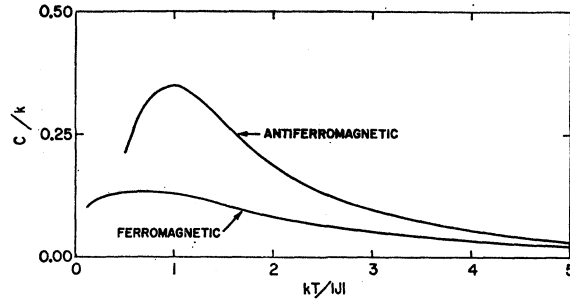


FIG. 5. Specific heat based on the $[11,10]$ Padé approximant for the ferromagnetic and the antiferromagnetic cases.

$K=1$, and is probably no more than ten percent off at $K = \infty$. The closest nonphysical singularities are at about $K = -0.11 \pm 0.47i$. The approximation to z based on the $[4,5]$ is

$$\begin{aligned} z(K) \approx & [(1 + 5.7979916K + 16.902653K^2 \\ & + 29.376885K^3 + 29.832959K^4 \\ & + 14.036918K^5) \div (1 + 2.7979916K \\ & + 7.0086780K^2 + 8.6538644K^3 + \\ & 4.5743114K^4)]^{2/3}. \end{aligned} \quad (3.9)$$

Since the energy is known¹² to tend to a finite limit as K tends to infinity and the values are known¹² to be

$$\lim_{K \rightarrow +\infty} E(K) = 1,$$

$$\lim_{K \rightarrow -\infty} E(K) = -4 \ln 2 + 1,$$

we have used the two-point Padé approximant method introduced in the previous section to analyze the energy. For the ferromagnetic case we have an error in the

¹² H. A. Bethe, *Z. Physik* **71**, 205 (1931); with A. Sommerfeld, *Handbuch der Physik*, edited by S. Flügge (Springer-Verlag, Berlin, 1933), Vol. 24, part 2, p. 618.

[9.9] of less than one part in 10^4 at $K=1$ and less than half a percent for $K=2$ at which point the value is 95% of the asymptotic value. Loss of calculational accuracy in the 20th coefficient prevents us from using the [10,10] where only about three places remain in the solution. When the standard Padé (one-point) approximant method is used, we may estimate E for $K=\infty$ to about 10% by averaging the twenty percent amplitude oscillation at $K=\infty$. The oscillation occurs because $K=\infty$ is an essential singularity. For $K<\infty$ agreement is rapidly obtained with the two-point method. It should be noted that the signs of the energy series are periodic with period 7, a rather long period. Consequently, a fairly large number of terms are required to obtain accurate results. The radius of convergence of the power series is about 0.5, the nearest singularities being located at about $-0.11\pm 0.47i$, the same place as for the reduced susceptibility. Unfortunately, the antiferromagnetic case is quite similar to the function $c(x)$ discussed in Sec. 2. There is again a cut which crosses the negative real axis in the neighborhood of

-2. We do, however, obtain the value at $K=-1$ to better than 3% accuracy and it is again about 95% of the asymptotic value for $K=-\infty$. In Fig. 4 we have plotted our results for the energy as a function of K .

We have compared our results with those obtained by Katsura and Inawashiro¹³ on the basis of an expansion through second order in J_{11} with J_{\perp} summed to all orders. The agreement for the antiferromagnetic energy is good. There is a deviation reaching about 6% in the range $K=0.2$ to 0.5. For the ferromagnetic energy the agreement is good for $K=0$ to 0.3 but starting around $K=0.3$ there is a large kink in their results which causes them to be off by about 20% near $K=1$ although their error drops to only 3% at $K=\infty$. Their ferromagnetic susceptibility agrees nicely with ours for $K=0$ to about 0.5 where theirs falls below ours due to the finiteness implicit in their approximation. In Fig. 5 we have plotted the specific heat at zero magnetic field as far as we believed our results to be reliable.

¹³ S. Katsura and S. Inawashiro (private communication).

Zero-Field Manganese Nuclear Magnetic Resonance in Antiferromagnetic Manganese Fluoride

E. D. JONES AND K. B. JEFFERTS

Bell Telephone Laboratories, Murray Hill, New Jersey

(Received 3 April 1964)

The zero-field NMR of Mn^{55} has been observed directly in the antiferromagnetic state of MnF_2 . A single resonance, with linewidth $\Delta\nu^{55}\approx 1.3$ Mc/sec, was observed in the frequency range of 650–675 Mc/sec and the temperature range of 1.3–20.5°K. The extrapolated Mn^{55} NMR frequency at 0°K is found to be $\nu_0^{55}=671.4\pm 0.2$ Mc/sec. Combining the 0°K Mn^{55} NMR frequency together with the dipolar field $H_{\text{dip}}=+5.770$ kOe and the hyperfine coupling constant $A^{55}=- (90.78\pm 0.3)\times 10^{-4}$ cm⁻¹, measured for Mn^{2+} in ZnF_2 , gives a value for the zero-point spin deviation of $1-\langle S \rangle/S = (0.43\pm 0.34)\%$. This value is to be compared with the value predicted by spin-wave theory of 2.37%. The observed temperature dependence of the Mn^{55} NMR frequency agrees, within experimental error, with the temperature dependence of the F^{19} zero-field NMR in antiferromagnetic MnF_2 . Upper and lower limits of 1300 kc/sec and 600 kc/sec are placed on the contribution to the Mn^{55} NMR linewidth in antiferromagnetic MnF_2 by the Suhl-Nakamura interaction.

I. INTRODUCTION

NUCLEAR magnetic resonance (NMR) techniques in antiferromagnetic media provide a convenient method for obtaining information about the thermodynamic properties of these ordered spin systems. In particular, information concerning the zero-point spin-deviation, temperature dependence of the sublattice magnetization, and indirect nuclear spin interactions are readily obtained from NMR measurements.¹ MnF_2 is a particularly well-suited crystal for

studying the properties of antiferromagnetic spin systems since the Mn^{2+} ion is an S -state ion ($S=5/2$) and therefore the anisotropy field results mainly from the dipolar interaction. MnF_2 has the rutile structure with tetragonal symmetry and in the antiferromagnetic state the Mn^{2+} ions are ordered such as to consist of two interpenetrating sublattices with oppositely ordered spins.

An estimate of the zero-point spin deviation $\langle S \rangle/S$ for MnF_2 has been given by Clogston *et al.*² by making a comparison of the electron paramagnetic resonance (EPR) measurements of Mn^{2+} in ZnF_2 with the specific

¹ For a review of NMR in antiferromagnetic media the reader is referred to the article by V. Jaccarino, in *Magnetism*, edited by H. Suhl and G. Rado (Academic Press Inc., New York, 1964).

² A. M. Clogston, J. P. Gordon, V. Jaccarino, M. Peter, and L. R. Walker, *Phys. Rev.* **117**, 1222 (1960).